# Iterative learning control for intermittently sampled data

Automatica 139 (2022) 110171

Contents lists available at ScienceDirect

Automatica

journal homepage: www.elsevier.com/locate/automatica

# Iterative learning control for intermittently sampled data: Monotonic convergence, design, and applications☆

Nard Strijbosch *, Tom Oomen

*Control Systems Technology Group, Department of Mechanical Engineering, Eindhoven University of Technology, The Netherlands*

ARTICLE INFO

*Article history:*
Received 21 May 2021
Received in revised form 22 October 2021
Accepted 23 December 2021
Available online 22 February 2022

*Keywords:*
Iterative learning control
Intermittent data
Incremental encoders

ABSTRACT

The standard assumption that a measurement signal is available at each sample in iterative learning control (ILC) is not always justified, e.g., when exploiting time-stamped data from incremental encoders or in systems with data dropouts. The aim of this paper is to develop a computationally tractable ILC framework that is capable of exploiting intermittent data while maintaining favourable properties, including monotonic convergence. A controllability and observability analysis of the intermittent ILC framework leads to appropriate monotonic convergence conditions which allow for missing data. These conditions lead to a new explicit ILC controller design independent of the sampling instances, which is reminiscent of gradient-descent ILC. The approach is demonstrated on both an intuitive example and a practically relevant example which exploits time-varying timestamped data from an incremental encoder.



## 1. Introduction

Iterative learning control (ILC) is being applied to achieve performance improvement of systems that are increasingly more complex. ILC exploits the reproducibility of the error when systems perform repeated tasks, see Bristow, Tharayil, and Alleyne (2006) for an introduction. After each repetition or iteration, the control action for the next iteration is improved by learning from the error observed in past iterations. Many successful applications have been reported, including additive manufacturing machines (Barton, Hoelzle, Alleyne, & Johnson, 2011; Hoelzle, Alleyne, & Johnson, 2010), robotic arms (Wallén, Norrlöf, & Gunnarsson, 2011), printing systems (Bolder, Oomen, Koekebakker, & Steinbuch, 2014), pick-and-place machines, electron microscopes (Strijbosch, Tacx, Verschueren, & Oomen, 2019), and wafer stages (Mishra, Coaplen, & Tomizuka, 2007; van der Meulen, Tousain, & Bosgra, 2008). Increasingly complex measurement signals can be exploited to update the control action including data from image processing, see, e.g., Bolder and Oomen (2016), Bolder et al. (2014), measurement signals at a different sampling rate compared to the control input, see, e.g., Oomen, van de Wijdeven, and Bosgra (2009), and non-equidistant sampled measurement signals, see, e.g., Shen (2018).

Typical ILC design approaches that have been successfully implemented have favourable properties including (1) an explicit learning update, instead of performing an optimization at each iteration, see Oomen and Rojas (2017) for details, and (2) achieving monotonic convergence in an appropriate norm of either the sequence of control inputs or the sequence of error signals (Longman, 2000; Son, Pipeleers, & Swevers, 2016). These properties are addressed in several existing approaches including frequency response function measurement data-based approaches, see, e.g., Blanken, van Zundert, de Rozario, Strijbosch, and Oomen (2019), Paszke, Rogers, Gałkowski, and Cai (2013), norm-optimal based approaches, see, e.g., Amann, Owens, and Rogers (1996), Chu and Owens (2009), Svante and Norrlöf (2001), and robust gradient-descent based ILC approaches, see, e.g., Bolder, Kleinendorst, and Oomen, Owens, Hatonen, and Daley (2009).

When only intermittent data is available, the standard assumption in ILC on the availability of exact measurement data at each sampling instance is violated. Intermittent observations of the error occur due to various (cyber-)physical phenomena, e.g., when non-equidistant but exact time-stamped data from incremental encoders is exploited (Strijbosch & Oomen, 2019a), data losses through data dropouts in networks (Ahn, Moore, & Chen, 2008; Shen & Wang, 2015b) and stealth attacks (Dan & Sandberg, 2010), or other constraints that prevent data

☆ This work is part of the research programme VIDI with project number 15698, which is (partly) financed by the Netherlands Organisation for Scientific Research (NWO). The material in this paper was presented at the 2019 American Control Conference (ACC), July 10–12, 2019, Philadelphia, PA, USA and the 58th IEEE Conference on Decision and Control, December 11–13, 2019, Nice, France. This paper was recommended for publication in revised form by Associate Editor Changyun Wen under the direction of Editor Miroslav Krstic.

* Corresponding author.
*E-mail addresses:* n.w.a.strijbosch@tue.nl (N. Strijbosch), t.a.e.oomen@tue.nl (T. Oomen).

https://doi.org/10.1016/j.automatica.2022.110171

transmission at each sampling instance (Altın & Sanfelice, 2018; Barton & Alleyne, 2011; Seel, Schauer, & Raisch, 2011).

Intermittent sampling phenomena occurring in complex (cyber-)physical systems have led to several different assumptions to model these intermittent observations for ILC, see e.g., Ahn et al. (2008), Shen and Wang (2015a). In Ahn et al. (2008), the availability of measurement data at each sampling instance is modelled by a probability density function. Another approach is to impose, for each measurement instance, a maximum is imposed on the number of consecutive iterations without data, see, e.g., Shen and Wang (2015a). All these modelling approaches impose assumptions on the availability of data. This probability distribution of available data or the maximum number of consecutive iterations are unknown in many applications. For instance, the time instances for which exact data from incremental encoders is available, also referred to as time-stamps, are directly related to the position (Strijbosch & Oomen, 2019a). In such cases, a worst-case analysis may be strongly preferred to provide guarantees for all possible realizations of available data.

Although several ILC approaches exist that allow for intermittent data, existing modelling approaches do not cover all possible (cyber-)physical phenomena that lead to intermittent data, and guarantees on monotonic convergence are not yet available. The aim of this paper is to develop a computationally tractable intermittent ILC framework with an explicit learning update that guarantees monotonic convergence in a worst-case setting. The developed ILC framework extends existing intermittent ILC approaches in Amann et al. (1996), Chu and Owens (2009), Svante and Norrlöf (2001) with (1) the possibility of modelling intersample data points and (2) a worst-case analysis and synthesis approach. This allows to design an ILC algorithm that exploits time-stamped data from incremental encoders for large-scale situations.

The main contribution of this paper is a computationally efficient intermittent ILC framework that guarantees monotonic convergence when limited error information is available at arbitrary time-varying measurement points. A unified intermittent ILC framework is presented, that encompasses a large number of applications, including quantization errors in incremental encoders. This is achieved through the following sub-contributions:

- C1 A worst-case analysis reveals intermittently sampling in ILC is not monotonically convergent in the classical sense. In addition, this is connected to controllability and observability of linear time-invariant (LTI) systems. See Section 3.
- C2 New subspace-based monotonic convergence definitions are introduced for intermittently sampled ILC. See Section 3.
- C3 A design framework is outlined leading to a single explicit learning update which is independent of the time instances with available data in an iteration. See Section 4.
- C4 A connection is established between the developed ILC approach and existing gradient-descent ILC design methods. This connection allows for an intuitive ILC design. See Section 5.

Finally, in Section 6, the ILC approach is demonstrated on both an intuitive example and a practically relevant example which exploits time-varying timestamped data from an incremental encoder. These results confirm monotonic convergence.

Very preliminary results related to the current manuscript are presented in Strijbosch and Oomen (2019a, 2019b). The present paper substantially extends preliminary results, including an extension of the monotonic convergence analysis to analyse monotonic convergence of the error, a theoretical analysis connecting the results to observability and controllability properties of LTI systems, and proofs. All proofs can be found in Appendix.

### 1.1. Notation and preamble

The spectral norm of a matrix $X \in \mathbb{R}^{n\times n}$ is given by $\rho(X) = \max_{i\in\{1,\ldots,n\}} |\lambda_i|$ where $\lambda_i$, $i \in \{1,\ldots,n\}$ are the eigenvalues of $X$. Let $A \in \mathbb{R}^{m\times n}$ and $B \in \mathbb{R}^{p\times q}$ then the Kronecker product of $A$ and $B$ is defined as

$$A \otimes B := \begin{bmatrix} a_{11}B & a_{12}B & \ldots & a_{1n}B \\ a_{21}B & a_{22}B & \ldots & a_{2n}B \\ \vdots & \vdots & & \vdots \\ a_{m1}B & a_{m2}B & \ldots & a_{mn}B \end{bmatrix} \in \mathbb{R}^{mp\times nq}. \tag{1}$$

The image of a matrix $A$, i.e., $\mathrm{im}(A)$, is given by the span of the columns of $A$. The induced norm of a matrix $A$ is defined as

$$\|A\|_{ip} = \max_{w\neq 0} \frac{\|Aw\|_p}{\|w\|_p} \tag{2}$$

where $\|w\|_p = \left(\sum_i |w_i|^p\right)^{(1/p)}$ denotes the vector $p$-norm, $p = 1, 2, \ldots$.

**Lemma 1.** *For any induced p-norm, $\rho(A) \leq \|A\|_{ip}$ (Skogestad & Postlethwaite, 2007).*

**Definition 1** (*Monotonic Convergence Towards a Fixed Point*)**.** A sequence $\{Y_j\}_{j\in\mathbb{Z}_{\geq 0}}$, $Y_j \in X$ converges monotonically, in the $p$-norm, $p \in \{1, 2, \ldots\}$, to a unique fixed point $Y_\infty \in X$, if there exists a $\kappa \in [0, 1)$ such that

$$\|Y_{j+1} - Y_\infty\|_p \leq \kappa \|Y_j - Y_\infty\|_p \tag{3}$$

is satisfied for all $Y_j \in X$, $j \in \mathbb{Z}_{\geq 0}$.

Consider strictly proper discrete-time linear time-invariant (LTI) systems described by

$$\begin{aligned} x(k+1) &= Ax(k) + Bu(k) \\ y(k) &= Cx(k) \end{aligned} \tag{4}$$

with state $x \in \mathbb{R}^{n_x}$, $n_x \in \mathbb{N}$, output $y \in \mathbb{R}^{n_y}$, $n_y \in \mathbb{N}$, and input $u \in \mathbb{R}^{n_u}$, $n_u \in \mathbb{N}$. The system matrices

$$\left[\begin{array}{c|c} A & B \\ \hline C & 0 \end{array}\right] \tag{5}$$

are of appropriate dimension. The Markov parameters of the system (4) are given by

$$m_k = \begin{cases} 0 \text{ if } k = 0 \\ CA^{k-1}B \text{ otherwise} \end{cases} \tag{6}$$

The pair $(A, B)$ in (4) is controllable if the controllable subspace $\mathcal{C} = \mathrm{im}\left(\begin{bmatrix} B & AB & \ldots & A^{n_x-1}B \end{bmatrix}^T\right)$ is full rank. This property implies that all eigenvalues of $A - BK$ can be freely assigned by an appropriate matrix $K \in \mathbb{R}^{n_u\times n_x}$, see, e.g., Zhou, Doyle, and Glover (1996, Theorem 3.1). Moreover, the system (4), or the pair $(A, B)$, is said to be stabilizable if every vector $x_c$ outside the controllable subspace $x_c \in \ker(\mathcal{C})$ has the property that $\lim_{k\to\infty} A^k x_c = 0$. This property implies that there exists a matrix $K \in \mathbb{R}^{n_u\times n_x}$ such that $\rho(A - BK) < 1$, see, e.g., Zhou et al. (1996, Theorem 3.2). Dual to controllability and stabilizability the pair $(A, C)$ is observable or detectable if the pair $(A^T, C^T)$ is controllable or stabilizable, respectively, see, e.g., Zhou et al. (1996, Theorem 3.3, Theorem 3.4).

## 2. Problem formulation with applications

In this section, the intermittently sampled ILC framework is presented. First, the ILC setup is introduced. Several application examples, including incremental encoders with time-stamped data, are shown to fit this formulation. Finally, the intermittently sampled ILC problem is formulated.

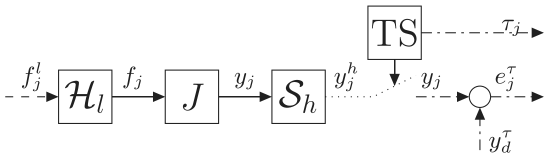


**Fig. 1.** Intermittently sampled ILC setup.

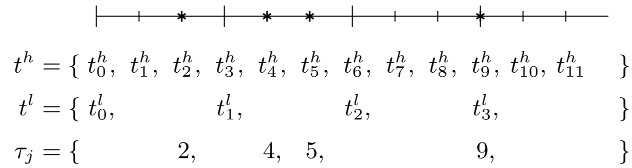


**Fig. 2.** Schematic representation of sets $t^h$, $t^l$ and $\tau_j$ with $M = 3$. The stars (*) indicate time-stamps during trial $j$.

### 2.1. ILC setup

The ILC setup that is considered consists of a continuous-time system $J$ of which the output is sampled at a high sample rate $h_h \in \mathbb{R}_{>0}$ and of a time-stamp generator (TS) that generates for each iteration a set of samples $\tau_j$ for which exact data is available.

The ILC setup is depicted in Fig. 1, where

$$y_j(t_c) = Jf_j(t_c), \tag{7}$$

and $J$ denotes a causal and stable continuous-time single-input single-output LTI system, which can be either an open-loop or closed-loop system. The index $j \in \mathbb{Z}_{\geq 0}$ denotes the $j$th task, and $t_c \in [0, T_c)$ denotes continuous-time, with $T_c \in \mathbb{R}$ the trial length. The following standard ILC assumption is imposed on the initial state of the system $J$.

**Assumption 1.** The initial condition of the system $J$ is identical for each iteration $j \in \mathbb{Z}_{\geq 0}$.

The ILC setup is implemented in a sampled-data setup, see Fig. 1, with an output sample time $h_h \in \mathbb{R}_{>0}$ and input sample time $h_l = Mh_h$, $M \in \mathbb{N}$. The ideal zero-order-hold $\mathcal{H}^l$ is used to interpolate the control input $f_j^l(t^l)$ as

$$\mathcal{H}^l : f_j(t_k^l + s) = f_j^l(k), \tag{8}$$

$s \in [0, h_l)$, $k \in \{0, \ldots, N^l - 1\}$, with

$$t_k^l = kh_l, \; k \in \{0, \ldots, N^l - 1\}. \tag{9}$$

The sampled output $y_j^h$ is obtained from the ideal sampler $\mathcal{S}^h$

$$\mathcal{S}^h : y_j^h(k) = y_j(t_k^h), \;\; k \in \{0, \ldots, N^h - 1\}, \tag{10}$$

with

$$t_k^h = kh_h, \; k \in \{0, \ldots, N^h - 1\}. \tag{11}$$

The desired trajectory is denoted by $y_d^h$.

**Assumption 2.** For the specific $y_d^h$ an input signal $f_d^l$ exists such that $y_d^h = \mathcal{S}^h J \mathcal{H}^l f_d^l$.

Assumption 2 states that $y_d^h$ is realizable, i.e., $e_j^h$ can be rendered zero.

The ILC setup is depicted in Fig. 1 and leads to the following sets of discrete-time sample instances.

**Definition 2.** The set of sampling instances of the control input $f_j^l$ is denoted by

$$t^l = \{t_0^l, t_1^l, \ldots, t_{N^l-1}^l\}, \; N^l \in \mathbb{N}. \tag{12}$$

**Definition 3.** The set of sampling instances of the output $y_j^h$ is denoted by

$$t^h = \{t_0^h, t_1^h, \ldots, t_{N^h-1}^h\}, \; N^h = MN^l. \tag{13}$$

Each trial, the time-stamp generator (TS) selects, depending on the application, a set of time stamps $\tau_j$ out of the set $t^h$. Each time stamp will refer to the sample number of the output at which data is available, and is defined as follows.

**Definition 4.** The set of time stamps is denoted by

$$\tau_j := \{\tau_{j,1}, \tau_{j,2}, \ldots, \tau_{j,N^{\tau_j}}\}, \tag{14}$$

where $\tau_{j,k} \in \{0, 1, \ldots, N^h - 1\}$ denotes the $k$th time-stamp in trial $j$. The value of $\tau_{j,k}$ refers to the sample number of the output at which the $k$th data point is available. Moreover, each time stamp satisfies the following

$$0 \leq \tau_{j,1} < \tau_{j,2} < \cdots < \tau_{j,N^{\tau_j}} \leq N^h - 1. \tag{15}$$

A schematic representation of a possible set $\tau_j$ and its relation to $t^h$ and $t^l$ is depicted in Fig. 2. The set of all possible sequences of observations is denoted by $\mathcal{T}$.

In this paper a worst-case analysis is of interest to develop guarantees for all possible sequences of observations. In other words, this will include the situation where in each iteration the worst-case sequence of observations is chosen. In the remainder of this paper it is assumed that the time-stamp generator chooses, for each iteration, the worst-case sequence of time-stamps from $\mathcal{T}$. The main benefit from this worst-case analysis is that it alleviates the necessity to model the availability of data, which is beneficial when considering, e.g., incremental encoders.

The goal of traditional ILC is to minimize the error at sample instances of the output $t^h$, i.e., $e^h$. To achieve this, each iteration $j$ the equidistantly sampled error $e_j^h$ is exploited to construct $f_{j+1}^l$ for the next iteration, i.e., $f_{j+1}^l = F(f_j^l, e_j^h)$.

**Remark 1.** Note that the standard ILC setup (Bristow et al., 2006) is recovered, when $\mathcal{T} = \{\bar{\tau}\}$, with $\bar{\tau}$ representing the set of time-stamps corresponding to the sample times of the control input, i.e., $\bar{\tau} = (0, M, 2M, \ldots)$.

In sharp contrast to Oomen et al. (2009), the considered problem in this paper is to exploit time-varying measurements in ILC, as is formulated next.

**Definition 5** (*Problem Formulation*)**.** Given the available data $e_j^{\tau_j}$ at the time-stamps $\tau_j$ develop a computationally tractable explicit ILC controller that minimizes the error between the output of system $J$ at the high rate sample instances $t^h$, i.e., $y_h$, and a desired output denoted by $y_d^h$, where the available error data to the ILC controller during iteration $j$ is given by

$$e_j^{\tau_j} = y_d^{\tau_j} - y_j^{\tau_j}. \tag{16}$$

### 2.2. Applications

In this section several applications that are captured by the ILC setup of Fig. 1 are exemplified. Systems vulnerable to data dropouts, see, e.g., Ahn et al. (2008), Shen and Wang (2015b), or stealth attacks, see, e.g., Dan and Sandberg (2010), fit naturally in the ILC setup given in Fig. 1, as the operator *TS* decides which data points are available. Moreover, systems that exploit incremental encoders to measure position, see e.g., Strijbosch and Oomen (2019a), are also captured by the ILC setup of Fig. 1, as explained in detail next.

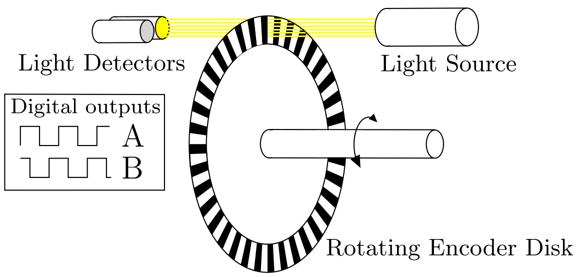


**Fig. 3.** Schematic representation of incremental encoder.

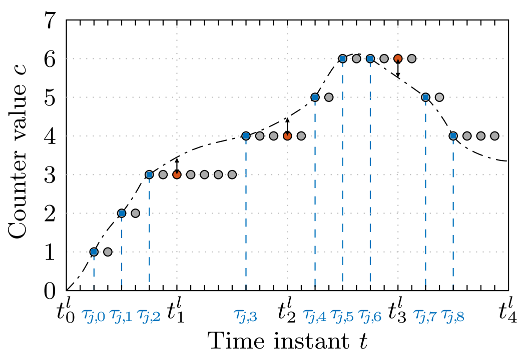


**Fig. 4.** The counter value of and incremental encoder corresponding to the position indicated by (-··-) The encoder operates at a very high equidistant sampling rate, indicated by the circles. The feedback control system operates at a lower equidistant sampling rate (●). Line-transitions are indicated by blue squares (■) and corresponding time-stamps $\tau_{j,k}$. These are exact, i.e., not subject to quantization error. In contrast, data points used by the feedback control system, clearly suffer from quantization, indicated by arrows (◂▸).

To illustrate that systems involving time-stamped data from incremental encoders are captured by the ILC setup of Fig. 1, the mechanical working principle of an incremental encoder is investigated. In Fig. 3, a schematic overview is presented of an incremental encoder. The main components are a slotted disc or strip, a light source and two light detectors. The light source is aimed at the light detectors. Depending on the position of the encoder disc the slots either obstruct the light or allow the light through. The output of the light detectors are two signals (A,B) which indicate if the light is perceived or not by the light detector.

The digital signals $(A, B)$ are in typical applications evaluated at a very high sampling rate $f_h = \frac{1}{h_h}$, $(\mathcal{O}(f_h) = 10^6 - 10^8$ Hz) (Merry, van de Molengraft, & Steinbuch, 2013). At each of these samples, it is determined if one of the signals changed, i.e., if a line transition occurred in between two time instances. A counter keeps track of the number of line transitions taking the direction into account. The width of the slots causes a quantization effect which must be addressed correctly (Salton, Fu, Flores, & Zheng, 2020).

Due to the high sampling rate $f_h$ compared to the number of line transitions per second, the difference between the time-instance of the line-transition and the time-stamp $\tau_{j,k}$ at the high sampling rate is negligible, i.e., the measurement $y^\tau_j[k]$ is exact, as exemplified in Fig. 4.

There are several ways to exploit the data from encoders in Fig. 4.

- The counter value at the equidistant sampling instances $t^l$ of the feedback system is exploited by the ILC algorithm. Since the sampling frequency of the feedback controller is limited by the real-time computations this approach leads to a quantization effect, indicated by (◂▸) in Fig. 4. If the quantization effect is modelled as an additional trial-varying noise term, it is consequently amplified by ILC (Oomen & Rojas, 2017; Svante & Norrlöf, 2001).
- The offline computations in ILC facilitate the employment of the non-equidistant data at the time stamps $\tau_j$, not corrupted by quantization, to obtain an increase in performance (Strijbosch & Oomen, 2019a).

The ILC setup as depicted in Fig. 1 encompasses the ILC setup that exploits time-stamped data from incremental encoders by taking the sampling frequency of the ideal sampler (10) equal to the sampling frequency of the encoder and by defining the operator $TS$ to define the time stamps based on the line-transitions.

## 3. Monotonic convergence: dealing with iteration-varying behaviour

In this section, it is shown that for an intermittently sampled ILC setup it is not possible to achieve monotonic convergence in the traditional sense of Definition 1. First, the finite time description of the intermittent ILC setup is introduced. Next, it is shown that the convergence analysis for the case where the time-stamp sequence is trial invariant is equivalent to a closed-loop analysis of the system (4). It turns out that controllability and observability of a discrete-time system of the form (4) allow for monotonic convergence. Specific time-stamp sequences may render the discrete-time system being uncontrollable and unobservable, preventing monotonic convergence, constituting Contribution C1. Finally, new monotonic convergence conditions are defined based on the controllable and unobservable subspaces, leading to Contribution C2.

### 3.1. Finite time description

A finite-time system description of the ILC setup of Fig. 1 is introduced. Consider the system $J^{h,h} = \mathcal{S}^h J \mathcal{H}^h$ with Markov parameters $m^h_k$, operating over a finite time interval $k \in \{0, \ldots, N^h\}$, where the system starts each trial with zero initial conditions. The input–output behaviour is represented by its convolution matrix $\underline{J}^{h,h} \in \mathbb{R}^{N^h \times N^h}$ which maps the input vector $\underline{f}^h_j \in \mathbb{R}^{N^h}$ to the output vector $\underline{y}^h_j \in \mathbb{R}^{N^h}$ (Frueh & Phan, 2000; Phan & Longman, 1988):

$$\underline{y}^h_j = \underline{J}^{h,h} \underline{f}^h_j, \quad \underline{J}^{h,h} = \begin{bmatrix} m^h_0 & & 0 \\ \vdots & \ddots & \\ m^h_{N^h-1} & \cdots & m^h_0 \end{bmatrix} \tag{17}$$

Define the finite-time description of the zero order hold $\mathcal{H}^{h,l}$ as $\underline{\mathcal{H}}^{h,l} = I_{N^l} \otimes \mathbb{I}_M$ with $\mathbb{I}_M := \left[1, \ldots, 1\right]^T \in \mathbb{R}^M$. Next, the finite-time description of $J^{h,l} = \mathcal{S}^h J \mathcal{H}^l$ is given by $\underline{J}^{h,l} = \underline{J}^{h,h} \underline{\mathcal{H}}^{h,l}$.

Moreover, define $\underline{T}_\tau \in \mathbb{R}^{N^\tau \times N^h}$ for all $\tau \in \mathcal{T}$, such that for each iteration $j$ the mapping from the error vector $\underline{e}^h_j \in \mathbb{R}^{N^h}$ to the error vector at the corresponding time-stamps $\underline{e}^{\tau_j}_j \in \mathbb{R}^{N^{\tau_j}}$ is given by

$$\underline{e}^{\tau_j}_j = \underline{T}_{\tau_j} \underline{e}^h_j, \quad \underline{T}_{\tau_j} = \begin{bmatrix} \epsilon^T_{\tau_{j,1}} & \epsilon^T_{\tau_{j,2}} & \cdots & \epsilon^T_{\tau_{j,N^{\tau_j}}} \end{bmatrix}^T, \tag{18}$$

where $\epsilon_{\tau_{j,k}}, k \in \{1, \ldots, N^{\tau_j}\}$ is a row vector of length $N_h$ with 1 in the $\tau_{j,k}$-th position and 0 in every other position.

The ILC update in iteration $j$ with time-stamp sequence $\tau_j \in \mathcal{T}$ is given by

$$\underline{f}^l_{j+1} = \underline{f}^l_j + \underline{L}_{\tau_j} \underline{e}^{\tau_j}_j \tag{19}$$

with $\underline{L}_{\tau_j} \in \mathbb{R}^{N^l \times N^{\tau_j}}$.

Using these definitions, the finite-time description of the intermittent ILC setup is given by

$$\begin{aligned} \underline{f}^l_{j+1} &= \underline{f}^l_j + \underline{L}_{\tau_j}\underline{e}^{\tau_j}_j, \\ \underline{e}^{\tau_j}_j &= \underline{T}_{\tau_j}\underline{y}^h_d - \underline{T}_{\tau_j}\underline{J}^{h,l}\underline{f}^l_j, \\ \tau_j &\in \mathcal{T}. \end{aligned} \tag{20}$$

The matrix $\underline{T}_{\tau_j}$ selects the rows from $\underline{J}^{h,l}$ that correspond that the time-stamp sequence $\tau_j$, leading to

$$\underline{J}_{\tau_j} = \underline{T}_{\tau_j}\underline{J}^{h,l} \tag{21}$$

in iteration $j$. Notice that the dimension of $\underline{J}_{\tau_j} \in \mathbb{R}^{N^{\tau_j}\times N^l}$ is iteration-varying. The ILC update (19) is therefore required to be iteration varying to accommodate this iteration varying dimension in $\underline{L}_{\tau_j}$. In the iteration invariant case, i.e., $\tau_j = \bar{\tau}$ for all $j \in \mathbb{Z}_{\geq 0}$, as in Remark 1, the finite-time ILC setup (20) reduces to the traditional case (Bristow et al., 2006).

### 3.2. Trial-invariant closed-loop analysis

Next, two discrete-time systems of the form (4) are derived for the iteration-invariant intermittent ILC setup (20) with time-stamp sequence $\tau_j = \tau_0$ for all $j \in \mathbb{Z}_{\geq 0}$ for some $\tau_0 \in \mathcal{T}$. First, convergence of the sequence of control inputs $\{\underline{f}^l_j\}_{j\in\mathbb{Z}_{\geq 0}}$ is analysed by considering $\underline{f}^l_j$ as state. Second, convergence of the sequence of error signals $\{\underline{e}^\tau_j\}_{j\in\mathbb{Z}_{\geq 0}}$ is analysed by considering $\underline{e}^\tau_j$ as state.

The ILC system (20) is recast into an LTI system state $\underline{f}^l_j$ as depicted in Fig. 5, where the system $S_f$ is given by

$$\begin{aligned} \underline{f}^l_{j+1} &= A_f\underline{f}^l_j + B_f\underline{v}^l_j \\ \underline{e}^{\tau_0}_j &= C_f\underline{f}^l_j, \end{aligned} \tag{22}$$

with input $\underline{v}^l_j := \underline{f}^l_{j+1} - \underline{f}^l_j$, output $\underline{e}^{\tau_0}_j$, and system matrices

$$\left[\begin{array}{c|c} A_f & B_f \\ \hline C_f & 0 \end{array}\right] = \left[\begin{array}{c|c} I_{N^l} & I_{N^l} \\ \hline -\underline{J}_{\tau_0} & 0 \end{array}\right]. \tag{23}$$

In this representation, the ILC controller is given by the static output feedback

$$\underline{v}^l_j = \underline{L}_{\tau_0}\underline{e}^{\tau_0}_j. \tag{24}$$

The closed-loop dynamics of (22) and (24) are given by

$$\underline{f}^l_{j+1} = \left(I_{N^l} - \underline{L}_{\tau_0}\underline{J}_{\tau_0}\right)\underline{f}^l_j + \underline{L}_{\tau_0}\underline{T}_{\tau_0}\underline{y}^h_d. \tag{25}$$

This leads to the following result.

**Lemma 2.** *Given the system description in (25), the sequence $\{\underline{f}^l_j\}_{j\in\mathbb{Z}_{\geq 0}}$ is convergent towards a unique $\underline{f}^l_\infty$, if and only if*

$$\rho\left(I_{N^l} - \underline{L}_{\tau_0}\underline{J}_{\tau_0}\right) < 1. \tag{26}$$

*Moreover, the sequence $\{\underline{f}^l_j\}_{j\in\mathbb{Z}_{\geq 0}}$ is monotonically convergent in a given p-norm if and only if*

$$\left\| I_{N^l} - \underline{L}_{\tau_0}\underline{J}_{\tau_0} \right\|_{ip} < 1. \tag{27}$$

Next, consider the convergence of the sequence of error signals $\{\underline{e}^{\tau_0}_j\}_{j\in\mathbb{Z}_{\geq 0}}$. Dual to (22) the ILC system (20) with $\tau_j = \tau_0$ for all $j \in \mathbb{Z}_{\geq 0}$ for some $\tau_0 \in \mathcal{T}$, is recast into an LTI system with state $\underline{e}^{\tau_0}_j$ as depicted in Fig. 6 where the system $S_e$ is given by

$$\begin{aligned} \underline{e}^{\tau_0}_{j+1} &= A_e\underline{e}^{\tau_0}_j + B_e\underline{v}^l_j, \\ \underline{e}^{\tau_0}_j &= C_e\underline{e}^{\tau_0}_j \end{aligned} \tag{28}$$

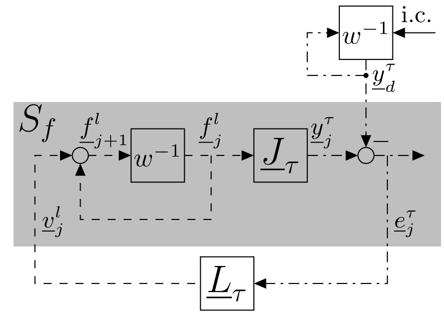


**Fig. 5.** ILC setup with state $\underline{f}^l_j$.

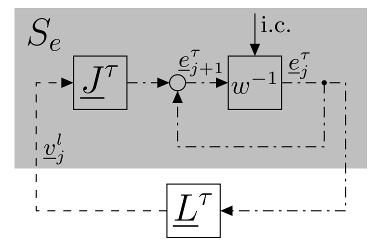


**Fig. 6.** ILC setup with state $\underline{e}^{\tau_j}_j$.

with input $\underline{v}^l_j$, output $\underline{e}^{\tau_0}_j$ and matrices $A_e = I_{N^{\tau_0}}$, $B_e = \underline{J}_{\tau_0}$, $C_f = I_{N^{\tau_0}}$. In this representation the ILC controller is given by (24).

The closed-loop dynamics of (28) and (24) are given by

$$\underline{e}^{\tau_0}_{j+1} = \left(I_{N^{\tau_0}} - \underline{J}_{\tau_0}\underline{L}_{\tau_0}\right)\underline{e}^{\tau_0}_j \tag{29}$$

This leads to the following Lemma.

**Lemma 3.** *Given the system description (29), the sequence $\{\underline{e}^{\tau_0}_j\}_{j\in\mathbb{Z}_{\geq 0}}$ is convergent towards a unique $\underline{e}^{\tau_0}_\infty$ if and only if*

$$\rho\left(I_{N^{\tau_0}} - \underline{J}_{\tau_0}\underline{L}_{\tau_0}\right) < 1. \tag{30}$$

*Moreover, the sequence $\{\underline{e}^{\tau_0}_j\}_{j\in\mathbb{Z}_{\geq 0}}$ is monotonically convergent in a given p-norm if and only if*

$$\left\| I_{N^{\tau_0}} - \underline{J}_{\tau_0}\underline{L}_{\tau_0} \right\|_{ip} < 1. \tag{31}$$

Lemmas 5 and 3 lead to conditions that guarantee the existence of a matrix $\underline{L}_{\tau_0}$ which are derived next.

### 3.3. Trial-invariant convergence: a controllability and observability perspective

The trial-domain dynamics (22) and (28) enable the design for convergence of the sequence of input signals $\{\underline{f}^l_j\}_{j\in\mathbb{Z}_{\geq 0}}$ or the sequence of error signals $\{\underline{e}^{\tau_j}_j\}_{j\in\mathbb{Z}_{\geq 0}}$, i.e., the possibility to design the matrix $\underline{L}_\tau$ such that either (26) or (30) is satisfied, from a controllability and observability perspective.

Consider the design of the ILC controller (19) to achieve convergence of the sequence of error signals $\{\underline{e}^{\tau_j}_j\}_{j\in\mathbb{Z}_{\geq 0}}$, i.e., design the matrix $\underline{L}_\tau$ for the system (28) such that (29) is stable. From the definition of stabilizability, it is concluded that this is only possible if the pair $(A_e, B_e)$ is stabilizable. Since all eigenvalues of $A_e$ are equal to 1, this is equivalent to controllability of the pair $(A_e, B_e)$. This leads to the following result (Contribution C1).

**Theorem 1.** *Consider the finite-time ILC setup (20) with trial-invariant time-stamp sequence, i.e. $\tau_j = \tau$ with $\tau \in \mathcal{T}$. Then, the following statement holds.*

*A An ILC update (19) exists that achieves a convergent sequence of errors $\{\underline{e}_j^{\tau_j}\}_{j\in\mathbb{Z}_{\geq 0}}$ if and only if*

$$\operatorname{rank}(\underline{J}_\tau) = N^\tau. \tag{32}$$

*In addition, Statement A implies the following*

*B. An ILC update (19) exists that achieves a monotonically convergent sequence of errors $\{\underline{e}_j^{\tau_j}\}_{j\in\mathbb{Z}_{\geq 0}}$ in any p-norm if and only if (32) is satisfied.*

Next, consider the design of the ILC update (19) to achieve convergence of the sequence of control inputs $\{\underline{f}_j^l\}_{j\in\mathbb{Z}_{\geq 0}}$, i.e., design the matrix $\underline{L}_\tau$ for the system (22) such that (25) is stable. Dual to the stabilizability of (28) for (22) detectability of $\underline{f}_j^l$ is required. Since all eigenvalues of $A_f$ are 1, this is equivalent to observability of the pair $(A_f, C_f)$. This leads to the following result (Contribution C1).

**Theorem 2.** *Consider the finite-time ILC setup (20) with trial-invariant time-stamp sequence, i.e. $\tau_j = \tau_0 \in \mathcal{T}$ for all $j \in \mathbb{Z}_{\geq 0}$. Then, the following statement holds.*

*A. An ILC update (19) exists that achieves a convergent sequence of input signals $\{\underline{f}_j^l\}_{j\in\mathbb{Z}_{\geq 0}}$ if and only if*

$$\ker(\underline{J}_\tau) = \{0\}. \tag{33}$$

*In addition, Statement A implies the following.*

*B. An ILC update (19) exists that achieves a monotonically convergent sequence of input signals $\{\underline{f}_j^l\}_{j\in\mathbb{Z}_{\geq 0}}$ if and only if (33) is satisfied.*

### 3.4. Trial-varying subspace-based monotonic convergence

The results in Theorems 1 and 2 show that there exist time-stamp sequences for which convergence in the traditional sense cannot be achieved, i.e., $\operatorname{rank}(\underline{J}_\tau) < N^l$ or $\operatorname{rank}(\underline{J}_\tau) < N^\tau$. Since the time-stamp generator chooses the worst-case time-stamp sequence for each iteration in a worst-case analysis, new monotonic convergence conditions are defined based on the unobservable and uncontrollable subspaces that consider all possible time-stamp sequences.

For the system (28), the controllable subspace is given by

$$\begin{aligned}\mathcal{C}_{S_e} &= \operatorname{im}\left(\begin{bmatrix} B_e & A_eB_e & \dots & A_e^{N^\tau-1}B_e\end{bmatrix}\right)\\ &= \operatorname{im}(\underline{J}_\tau).\end{aligned} \tag{34}$$

Given this subspace the error can be decomposed into a controllable and uncontrollable part, given in the following definition.

**Definition 6.** Given the controllable subspace (34), the error $\underline{e}_j^{\tau_j}$ can be decomposed into a controllable part $\underline{e}_{j,c_j}^{\tau_j}$, and uncontrollable part $\underline{e}_{j,uc_j}^{\tau_j}$, i.e.,

$$\underline{e}_j^{\tau_j} = \underline{e}_{j,c_j}^{\tau_j} + \underline{e}_{j,uc_j}^{\tau_j} \tag{35}$$

where $\underline{e}_{j,c_j}^{\tau_j} \subset \operatorname{im}(\underline{J}_\tau)$.

The error in the controllable subspace, $\underline{e}_{j,c_j}^{\tau_j}$, can converge by an appropriate design of the ILC law (19), i.e., all eigenvalues of the system matrix $A_e$ corresponding to this subspace can be placed inside the unit disc by the feedback (24).

The following example reveals how the uncontrollable part of the error behaves.

**Example 1.** Consider the ILC setup (20) with trial-invariant time-stamp sequence $\tau \in \mathcal{T}$ with corresponding convolution matrix and learning matrix

$$\underline{J}_\tau = \begin{bmatrix} 0 & 0 & 0\\ 1 & 0 & 0\\ -1 & 1 & 0\end{bmatrix}, \underline{L}_\tau = \begin{bmatrix} l_{11} & l_{12} & l_{13}\\ l_{21} & l_{22} & l_{23}\\ l_{31} & l_{32} & l_{33}\end{bmatrix}. \tag{36}$$

This yields the closed-loop error dynamics (29) given by

$$\underline{e}_{j+1}^\tau = \begin{bmatrix} 1 & 0 & 0\\ * & * & *\\ * & * & *\end{bmatrix}\underline{e}_j^{\tau_j} \tag{37}$$

where the values depending on $\underline{L}_\tau$ are denoted by $*$. This corresponds to the controllable subspace given by

$$\operatorname{im}(\mathcal{C}_{S_e}) = \operatorname{im}(\underline{J}_\tau) = \operatorname{span}\left(\begin{bmatrix}0\\1\\0\end{bmatrix}, \begin{bmatrix}0\\0\\1\end{bmatrix}\right). \tag{38}$$

From which it follows that the first element of $\underline{e}_j^\tau$ cannot be influenced by the ILC controller. Both the second and third element follow dynamics influenced by the feedback (24).

This behaviour is caused by the part of the error which is not controllable and therefore cannot be affected by the input $\underline{f}_j^l$. This uncontrollable part of the error follows the free response dictated by $A_e = I_{N^\tau}$, i.e.,

$$\underline{e}_{j+1,uc_j}^{\tau_j} = \underline{e}_{j,uc_j}^{\tau_j}. \tag{39}$$

In the trial-varying ILC setup, the controllable subspace is trial-varying. To accommodate a monotonic convergence analysis of the sequence of errors $\{\underline{e}_j^h\}_{j\in\mathbb{Z}_{\geq 0}}$ in a worst-case setting, the following monotonic convergence condition is introduced, leading to Contribution C2.

**Definition 7** (*Intermittent Monotonic Convergence of the Error*)**.** The sequence of error signals $\{\underline{e}_j^h\}_{j\in\mathbb{Z}_{\geq 0}}$ of the ILC setup with intermittent time-varying measurement points is called monotonically convergent in a given $p$-norm if there exists a $\kappa_c \in [0, 1)$ such that

$$\|\underline{e}_{j+1,c_j}^h - \underline{e}_{d,c_j}^h\|_p \leq \kappa_c \|\underline{e}_{j,c_j}^h - \underline{e}_{d,c_j}^h\|_p. \tag{40}$$

In addition, the

$$\|\underline{e}_{j+1}^h - \underline{e}_d^h\|_p \leq \kappa_{tot}\|\underline{e}_j^h - \underline{e}_d^h\|_p, \tag{41}$$

should be satisfied for some $\kappa_{tot} \in [0, 1]$. To guarantee that the uncontrollable part of the error is monotonically non-increasing.

**Remark 2.** Note that the notion of an error for $j \to \infty$ does not exist for Definition 7, since there could exist a part of the error that is uncontrollable for each iteration $j \in \mathbb{Z}_{\geq 0}$. Thereby this part of the error cannot be altered by the ILC, while still satisfying (41).

From Definition 7, conditions can be derived to check if a given intermittent ILC controller (19) with matrices $\underline{L}_\tau$, for all $\tau \in \mathcal{T}$ leads to a monotonically convergent sequence of control inputs $\{\underline{e}_j^h\}_{j\in\mathbb{Z}_{\geq 0}}$ in the 2-norm, given by the following result.

**Lemma 4.** *Consider the finite-time trial-varying intermittent ILC system (20) satisfying Assumption 2. The sequence of control inputs $\{\underline{e}_j^h\}_{j\in\mathbb{Z}_{\geq 0}}$ is monotonically convergent in the 2-norm towards the fixed point $\underline{e}^h = 0$ as in Definition 7, if and only if for each $\tau \in \mathcal{T}$*

$$\left\| I_{N^{c_j}} - U_{1,\tau}^T \underline{J}_\tau \underline{L}_\tau U_{1,\tau}\right\|_{i2} < 1, \tag{42}$$

*where $U_{1,\tau} \in \mathbb{R}^{N^h \times (N^{c_j})}$ is constructed from a singular value decomposition of $\underline{J}_\tau$ as in Lemma 6, and*

$$\left\| I_{N^h} - \underline{J}_\tau \underline{L}_\tau \right\|_{i2} \leq 1. \tag{43}$$

Dual to the controllable subspace of system (28) the unobservable subspace of system (22) is given by

$$\mathcal{O}_{S_f} = \ker\left(\begin{bmatrix} C_f \\ C_f A_f \\ \vdots \\ C_f A_e^{N^\tau - 1} \end{bmatrix}\right) = \ker(\underline{J}_\tau) = 0. \tag{44}$$

Given this subspace the control input $\underline{f}_j^l$ can be decomposed into an observable and unobservable part, given in the following definition.

**Definition 8.** Given the unobservable subspace (44) the control input $\underline{f}_j^l$ can be decomposed into an observable part, $\underline{f}_{j,\mathrm{o}}^l$, and unobservable part $\underline{f}_{j,\mathrm{uo}}^l$, i.e.

$$\underline{f}_j^l = \underline{f}_{j,\mathrm{o}}^l + \underline{f}_{j,\mathrm{uo}}^l \tag{45}$$

where $\underline{f}_{j,\mathrm{uo}}^l \in \ker(\underline{J}_\tau)$.

To accommodate a monotonic convergence analysis of the sequence of errors $\{\underline{f}_j^l\}_{j\in\mathbb{Z}_{\geq 0}}$ in a worst-case setting, the following monotonic convergence condition is introduced, leading to Contribution C2.

**Definition 9** (*Intermittent Monotonic Convergence of the Input*)**.** The sequence of input signals $\{\underline{f}_j^l\}_{j\in\mathbb{Z}_{\geq 0}}$ of the ILC setup with intermittent time-varying measurement points is called monotonically convergent in a given $p$-norm if there exists a $\kappa_\mathrm{o} \in [0, 1)$ such that

$$\|\underline{f}_{j+1,\mathrm{o}_j}^l - \underline{f}_{d,\mathrm{o}_j}^l\|_p \leq \kappa_\mathrm{o} \|\underline{f}_{j,\mathrm{o}_j}^l - \underline{f}_{d,\mathrm{o}_j}^l\|_p. \tag{46}$$

In addition,

$$\|\underline{f}_{j+1}^l - \underline{f}_d^l\|_p \leq \kappa_\mathrm{tot} \|\underline{f}_j^l - \underline{f}_d^l\|_p, \tag{47}$$

should be satisfied for some $\kappa_\mathrm{tot} \in [0, 1]$, to guarantee that the unobservable part of the control input is monotone non-increasing.

From Definition 9, conditions can be derived to check if a given intermittent ILC controller (19) with matrices $\underline{L}_\tau$, for all $\tau \in \mathcal{T}$ leads to a monotonically convergent sequence of control inputs $\{\underline{f}_j^l\}_{j\in\mathbb{Z}_{\geq 0}}$ in the 2-norm, given by the following result.

**Lemma 5.** *Consider the finite-time trial-varying intermittent ILC system (20) satisfying Assumption 2. The sequence of control inputs $\{\underline{f}_j^l\}_{j\in\mathbb{Z}_{\geq 0}}$ is monotonically convergent in the 2-norm towards the fixed point $\underline{f}_d^l$ as in Definition 9, if and only if for each $\tau \in \mathcal{T}$*

$$\left\| I_{N^l - N^{o_j}} - V_{1,\tau}^T \underline{L}_\tau \underline{J}_\tau V_{1,\tau} \right\|_{i2} < 1, \tag{48}$$

*where $V_{1,\tau} \in \mathbb{R}^{N^l \times (N^l - N^{o_j})}$ is constructed from a singular value decomposition of $\underline{J}_\tau$ as in Lemma 6, and*

$$\left\| I_{N^l} - \underline{L}_\tau \underline{J}_\tau \right\|_{i2} \leq 1. \tag{49}$$

This result is exploited in the next section to develop a computationally tractable intermittent ILC design approach.

## 4. Computationally tractable ILC approach

In this section, a computationally tractable ILC approach is developed to design (19) for the ILC setup presented in Fig. 1. From Lemma 5, a necessary structure is derived for the ILC controller to guarantee monotonic convergence of the sequence of control inputs $\{\underline{f}_j^l\}_{j\in\mathbb{Z}_{\geq 0}}$ in the 2-norm. This structure is exploited to develop an explicit ILC approach that is independent of the size of $\mathcal{T}$, leading to Contribution C3.

### 4.1. Monotonic convergence in the 2-norm

First, a structure for the matrix $\underline{L}_\tau$ is derived that is necessary to achieve monotonic convergence of the sequence of control inputs $\{\underline{f}_j^l\}_{j\in\mathbb{Z}_{\geq 0}}$ as in Definition 9.

**Theorem 3.** *Consider the finite-time time-stamped ILC system (20) satisfying Assumption 2. Then it is necessary that each matrix $\underline{L}_\tau$, $\tau \in \mathcal{T}$, satisfies*

$$\underline{L}_\tau \in \mathrm{im}\,\underline{J}_\tau^T. \tag{50}$$

*to obtain a monotonically convergent sequence of control inputs $\{\underline{f}_j^l\}_{j\in\mathbb{Z}_{\geq 0}}$ in the 2-norm towards the fixed point $\underline{f}_d^l$ as in Definition 9. In addition, if Condition (48) is satisfied for all $\tau \in \mathcal{T}$ with matrices $\underline{L}_\tau$, $\tau \in \mathcal{T}$ of the form (50), Condition (49) is automatically guaranteed.*

This result shows that the design problem to find the set of matrices $\underline{L}_\tau$, $\tau \in \mathcal{T}$ is reduced to finding matrices of the form (50) that satisfy (48). Since, all matrices that satisfy (50) can be characterized by $\underline{J}_\tau^\top \underline{X}_\tau$ for some $\underline{X}_\tau \in \mathbb{R}^{N^h \times N^\tau}$, it is concluded the intermittent ILC design problem can be reduced to finding for each $\tau \in \mathcal{T}$ a matrix $\underline{X}_\tau \in \mathbb{R}^{N^h \times N^\tau}$ such that Condition (48) is satisfied with

$$\underline{L}_\tau = \underline{J}_\tau^\top \underline{X}_\tau. \tag{51}$$

### 4.2. Explicit ILC controller

Next, the result of Theorem 3 is exploited to obtain a computationally efficient design approach in which only a single matrix should be designed instead of a matrix for each $\tau \in \mathcal{T}$, leading to Contribution C3 of this paper. For this, the matrix

$$\underline{L}_\tau = \underline{L}\underline{T}_\tau, \tag{52}$$

is introduced for each $\tau \in \mathcal{T}$ with $\underline{L} \in \mathbb{R}^{N^l \times N^h}$ to reduce the design of the ILC law (19) to finding only the single matrix $\underline{L}$. This reduces the computation time significantly. However, it should be noted that this reduction in design variables for the ILC update law potentially results in a slower convergence rate.

Exploiting Theorem 3, the following result is obtained for the ILC controller given by (19) with (52).

**Theorem 4** (*Explicit ILC Controller*)**.** *Consider the finite-time time-stamped ILC system (20) with desired output $\underline{y}_d^h$ satisfying Assumption 2 and the ILC controller of the form (19) with (52). The sequence of control inputs $\{\underline{f}_j^l\}_{j\in\mathbb{Z}_{\geq 0}}$ of (20) converges monotonically towards $\underline{f}_d^l$, in the 2-norm, if and only if $\underline{L}$ is given by*

$$\underline{L} := (\underline{J}^{h,l})^T \underline{D} \tag{53}$$

*with $\underline{D} \in \mathbb{R}^{N^h \times N^h}$ a diagonal matrix with positive entries that satisfies the following linear matrix inequality (LMI)*

$$2I_{N^l} - (\underline{J}^{h,l})^T \underline{D} \underline{J}^{h,l} \succ 0. \tag{54}$$

From this result it follows that the design of an intermittent ILC controller that guarantees monotonic convergence of the sequence of control inputs can be reduced to finding a single diagonal matrix $\underline{D}$ that satisfies a single LMI. The size of this LMI is

$N^l \times N^l$ and can therefore easily be verified for a given matrix $\underline{D}$ or used in a semidefinite program (SDP) to find an optimal matrix $\underline{D}$ for a given cost function. This design method is independent of the size of $\mathcal{T}$, thereby resulting in a computationally efficient approach.

## 5. Connection to gradient-descent ILC

In this section, a connection is established between the ILC approach resulting from Theorem 4 and the gradient-descent ILC design method in Bolder et al., Owens et al. (2009). This connection allows for intuitive guidelines to design the matrix $D$, leading to contribution C4 of this paper.

### 5.1. Gradient-descent ILC

In gradient-descent ILC (Bolder et al.; Owens et al., 2009), an iteration invariant ILC system is considered with finite-time description

$$\underline{e}_j = \underline{y}_d - \underline{J}\underline{f}_j. \tag{55}$$

The performance of the ILC algorithm is given by the cost function $\mathcal{J}(\underline{f}_{j+1}) = \underline{e}_{j+1}{}^T W_e \underline{e}_{j+1}$ with $W_e \succeq 0$ a user defined weighting matrix. The error at iteration $j+1$ can be written as $\underline{e}_{j+1} = \underline{e}_j + \underline{J}(\underline{f}_j - \underline{f}_{j+1})$ using (55). This leads to the gradient of $\mathcal{J}(\underline{f}_{j+1})$ with respect to $\underline{f}_{j+1}$, given by

$$\frac{\partial \mathcal{J}(\underline{f}_{j+1})}{\partial \underline{f}_{j+1}} = 2\underline{J}^T W_e \underline{J}(\underline{f}_{j+1} - \underline{f}_j) - 2\underline{J}^T W_e \underline{e}_j. \tag{56}$$

The learning update is given by choosing a control input in the steepest descent direction, i.e.,

$$\underline{f}_{j+1} = \underline{f}_j - \varepsilon \left. \frac{\partial \mathcal{J}(\underline{f}_{j+1})}{\partial \underline{f}_{j+1}} \right|_{\underline{f}_{j+1} = \underline{f}_j} = \underline{f}_j + 2\varepsilon \underline{J}^T W_e \underline{e}_j, \tag{57}$$

where $\varepsilon \in \mathbb{R}_{>0}$ determines the size of the step in the steepest descent direction. Choosing the step $\varepsilon$ sufficiently small ensures that the cost function decays in each iteration, see Bolder et al., Owens et al. (2009), which leads to a decrease of the criterion $\mathcal{J}$.

### 5.2. Connection to ILC approach in Theorem 4

The learning update for the ILC setup (20) with (19) and (53) is given by

$$\underline{f}_{j+1} = \underline{f}_j + \underline{J}^{h,l^T} D \underline{T}_{\tau_j}^T \underline{T}_{\tau_j} \underline{e}_j. \tag{58}$$

Note that this learning update is equivalent to the update law (57), with $2\varepsilon W_e := D\underline{T}_{\tau_j}^T \underline{T}_{\tau_j} \succeq 0$. Therefore, the learning update (58) at trial $j$ is equivalent to a steepest descent update with cost function $\mathcal{J}_{\tau_j}(\underline{f}_{j+1}) = \underline{e}_{j+1}{}^T D \underline{T}_{\tau_j}^T \underline{T}_{\tau_j} \underline{e}_{j+1}$. Each of the cost functions $\mathcal{J}_{\tau_j}(\underline{f}_{j+1})$ is convex with the point $\underline{f}_{j+1}^l = \underline{f}_d^l$ in its optimum.

The above observations allow the design of the matrix $D$ to be equivalent to the intuitive design of a weighting matrix $W_e$ which is extensively studied in the literature (Bristow et al., 2006). By choosing $D = \alpha W_e$ with $W_e \in \mathbb{R}^{N_h \times N_h}$ a diagonal matrix with positive entries and a sufficiently small $\alpha \in \mathbb{R}_{>0}$ to satisfy (54) leads to monotonic convergence as in Definition 9.

## 6. Examples

In this section, the explicit ILC controller introduced in Section 4 is applied to two examples. First, an intuitive example is introduced with $f^h = f^l$ and trial length, $N^h = 3$. This example allows to clearly observe the time stamp sequences $\tau_j$. Next, a practically relevant example of a mass–spring–damper system and trial length of $N^h = 2000$ is introduced. This trial length leads to $2^{2000}$ possible time-stamp sequences, i.e., a computationally tractable ILC controller as introduced in Section 4 is a necessity.

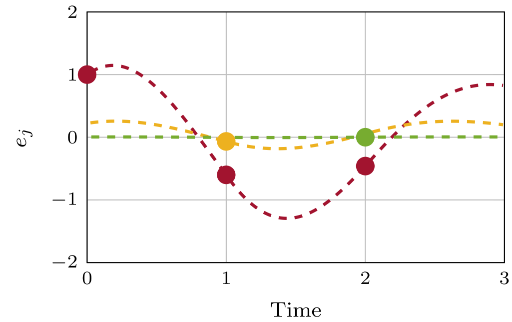


Fig. 7. Error $e_j^h$ at trial $j = 0$ (- -), $j = 10$ (- -), and $j = 40$ (- -) when applying an intermittent ILC controller of Theorem 4 with the available error at the time-stamps, $\underline{e}_j^\tau$ indicated by dots (●).

### 6.1. Intuitive example

The system considered in this example has the following convolution matrix

$$\underline{J}^{h,l} = \begin{bmatrix} 1 & 0 & 0 \\ 0.4 & 1 & 0 \\ -0.56 & 0.4 & 1 \end{bmatrix}. \tag{59}$$

The aim of this example is to find an input $\underline{f}^l$ such that $\underline{y}_j^h$ converges towards the desired position $\underline{y}_d^h = \begin{bmatrix} 1 & -0.6 & -0.46 \end{bmatrix}^T$. For each iteration $j$ the time-stamp sequences $\tau_j$ are randomly selected from all possible time-stamp sequences $\mathcal{T}$. Three ILC controllers are compared: (1) The ideal case where for each iteration all measurement instances are available, i.e., $\tau_j = \{0, 1, 2\}$ for all $j \in \mathbb{Z}_{\geq 0}$, with $\underline{L}_{\tau_j} = \epsilon \underline{J}^{h,l^T}$ for each $j \in \mathbb{Z}_{\geq 0}$; (2) an intermittently sampled ILC controller (51), i.e., for each possible $\tau \in \mathcal{T}$ a matrix $\underline{L}_\tau$ is determined as $\underline{L} = \epsilon_\tau \underline{J}^T$; (3) A computationally tractable intermittently sampled ILC controller (52) which is designed exploiting Theorem 4 with $D = 0.5 I_{N^h}$.

In Fig. 8, the error norm $\|e_j^h\|_2$ is given from which it is observed that each of the ILC controller leads to increased performance. Moreover, from Fig. 9 it is concluded that the sequence of control inputs converges monotonically towards $f_d^l$ in the 2-norm. The ILC controller that can exploit measurement data at each sample instance converges at the highest rate. The extra design freedom of the ILC controller (51) enables a slightly higher convergence rate compared to the computationally tractable ILC controller (52).

From Fig. 7 it is clear that the data used by the intermittent ILC controller is non-equidistant in time and trial-varying. Nonetheless, from Fig. 8 and Fig. 9 it can be observed that the intermittent ILC controller leads to convergence in both the error and control-input. In Fig. 8, the error norm $\|e_j^h\|_2$ is shown when applying traditional ILC with full error information and when applying the intermittent ILC controller. From Fig. 8, it is observed that both methods achieve convergence towards $\|e_\infty^h\|^2 = 0$. From Fig. 9 it is observed that for both methods monotonic convergence of the control input towards $f_d^l$ is achieved in the 2 norm.

### 6.2. Practically relevant example

In this example a mass–spring–damper system is considered with the following transfer function

$$J(s) = \frac{1}{ms^2 + cs + k} \tag{60}$$

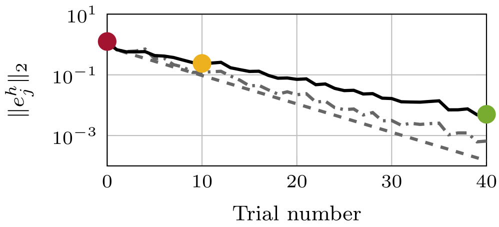


**Fig. 8.** Error norm $\|e_j^h\|_2$ when applying an intermittent ILC controller designed following Theorem 4 (—), and Theorem 3 (– · –). The situation where all data is available at each trial $j$ (– –). The error norm $\|e_j^h\|_2$ of trails $j \in \{0, 10, 40\}$ as depicted in Fig. 7 are highlighted with their corresponding colour.

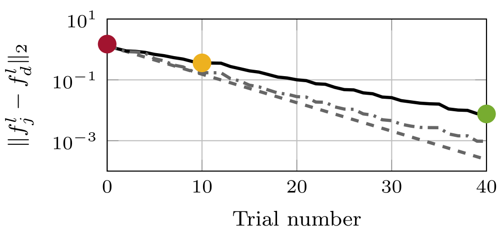


**Fig. 9.** Input difference norm $\|f_j^l - f_d^l\|_2$ when applying an intermittent ILC controller designed following Theorem 4 (—), and Theorem 3 (– · –). The situation where all data is available at each trial $j$ (– –). The norm $\|f_j^l - f_d^l\|_2$ of trails $j \in \{0, 10, 40\}$ as depicted in Fig. 7 are highlighted with their corresponding colour.

with mass $m = 1$ [kg], damping coefficient $c = 10$ [N m/s], and spring constant $k = 100$ [N/m] is considered. The position of the mass is measured by an incremental encoder with an accuracy of $5 \cdot 10^{-4}$ [m]. The sampling frequencies of the control input and encoder are, $h_l = 1 \cdot 10^{-2}$ [s] and $h_h = 1 \cdot 10^{-3}$ [s], respectively. The aim of this example is to find an input $f^l$ such that the position of the mass follows the 4th order reference $y_d^h$, of which a scaled version is given by the dashed–dotted line in Fig. 10.

A traditional ILC controller exploiting equidistant data and an explicit intermittent ILC controller (52) are designed using the finite-time description as discussed in Section 3. The traditional ILC controller exploits the counter data available at the sampling instances of the control input, $t_k^l$, thereby introducing a quantization effect as explained in Section 2. This traditional quantized ILC controller is given by (19) with $\underline{L}_{\tau_0} = (J^{l,l})^{\dagger}$. The decentralized ILC controller that exploits the exact data that is available at the time stamps, is determined using Theorem 4. For this application, the error at each sample is considered to be of equal importance, this corresponds to a weighting filter $W_e = I_{N^h}$. Hence, the matrix $D$ is designed as $\epsilon I_{N^h}$. The value of $\epsilon$ is chosen as $\epsilon = (\|\underline{J}^{h,l^T} \underline{J}^{h,l}\|_{i2})^{-1}$ to satisfy Condition (54).

In Fig. 11, the error norm $\|e_j^h\|_2$ is shown when applying traditional ILC with quantized data and when applying the intermittent ILC controller. From Fig. 11, it is observed that the intermittent ILC controller achieves higher performance, as the error norm $\|e_j^h\|_2$ of intermittent ILC reaches a lower value compared to traditional quantized ILC. This can also be observed in Fig. 10, where the error of both ILC approaches after 750 trials is presented. In Fig. 10 it is observed that the error resulting from intermittent ILC reduces to below the encoder resolution. It is also observed that the data used by the intermittent ILC controller is non-equidistant in time. In Fig. 12, the monotonic convergence property of the sequence of input signals in the 2-norm is evaluated for both ILC approaches. From Fig. 12 it is observed that when exploiting traditional ILC with quantized data convergence of the control input towards $f_d^l$ is not achieved, where the control input of intermittent ILC converges monotonically towards $f_d^l$.

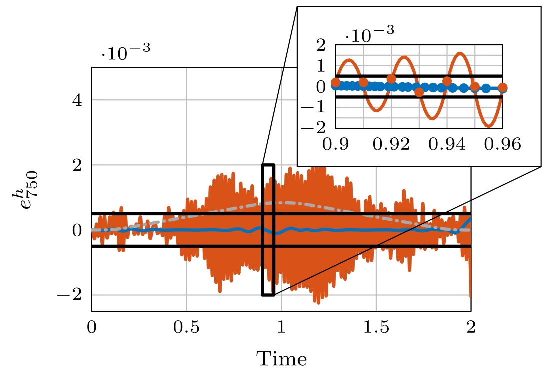


**Fig. 10.** Error $e_{750}^h$ at trial 750 after applying traditional ILC with quantized data (—) and after applying intermittent ILC controller of Theorem 4 with exact data at the time-stamps (—). In the zoom the time-instances of the available error data are indicated by dots (● and ●). The quantization level is indicated by (—). The dash-dotted line (– · –) depicts the reference scaled down by a factor 400.

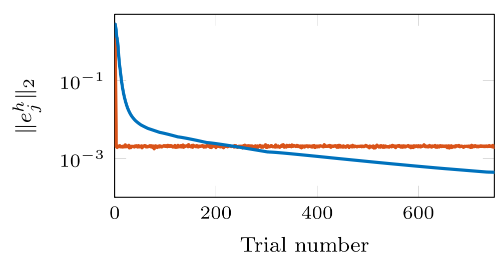


**Fig. 11.** Error norm $\|e_j^h\|_2$ when applying traditional ILC using quantized data (—) and when applying the intermittent ILC controller of Theorem 4 (—).

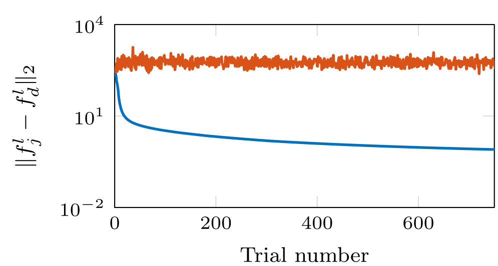


**Fig. 12.** Norm $\|f_j^l - f_d^l\|_2$ when applying traditional ILC with quantized data (—) and when applying the intermittent ILC controller of Theorem 4 (—).

## 7. Conclusions

All error knowledge should be used to improve control performance to the limit, which is precisely the approach intermittent ILC takes. For example for system that exploits incremental encoders intermittently sampled ILC allows for a performance increase for existing systems due to the use of exact data instead of quantized data, or it could come with cost benefits since cheaper sensors with a higher quantization level could lead to similar performance levels. A new framework exploiting a single explicit ILC controller for intermittent ILC is developed that guarantees monotonic convergence without imposing any assumptions on the availability of data through a worst-case analysis. This immediately allows large scale implementation of various relevant applications with intermittent observations, including systems with incremental encoders, and systems with networked or stealth attack issues. It is shown that due to the trial varying availability of the output, monotonic convergence in its standard definition cannot be obtained. A new subspace-based definition for monotonic convergence for this type of systems is introduced. A computationally efficient design procedure for an

ILC algorithm that guarantees monotonic convergence is developed. A connection is established between the developed design procedure and the existing gradient-descent ILC approach leading to an intuitive design procedure. The developed design procedure is applied to two examples confirming monotonic convergence.

## Appendix

**Lemma 6.** *Consider a matrix $A \in \mathbb{R}^{m\times n}$ with $\operatorname{rank}(A) = k < \min(m,n)$. Consider the singular value decomposition of A, given by*

$$A = U\begin{bmatrix}\Sigma & 0\\ 0 & 0\end{bmatrix}V^\top = \begin{bmatrix}U_1 & U_2\end{bmatrix}\begin{bmatrix}\Sigma & 0\\ 0 & 0\end{bmatrix}\begin{bmatrix}V_1^\top\\ V_2^\top\end{bmatrix} \tag{A.1}$$

*with $\Sigma \in \mathbb{R}^{k\times k}$ a diagonal matrix with strictly positive entries, and orthonormal matrices $U \in \mathbb{R}^{m\times m}$, $V \in \mathbb{R}^{n\times n}$. Moreover, $U_1 \in \mathbb{R}^{m\times k}$, $U_2 \in \mathbb{R}^{m\times(m-k)}$, $V_1 \in \mathbb{R}^{n\times k}$, and $V_2 \in \mathbb{R}^{n\times k-n}$. Then the following subspaces are equivalent (Skogestad & Postlethwaite, 2007)*

$$\operatorname{im} A^T = \operatorname{im} V_1, \text{ and } \ker A = \operatorname{im} V_2. \tag{A.2}$$

**Lemma 7.** *Consider a matrix $X \in \mathbb{R}^{m\times n}$ and $\operatorname{rank}(X) = m$, and the diagonal matrix $D \in \mathbb{R}^{n\times n}$. When $n = m$ then $XDX^T \succ 0$ if and only if the matrix $D \succ 0$ (Bernstein, 2009). Moreover, if $m < n$, then $XDX^T \succ 0$ if $D \succ 0$.*

**Lemma 8.** *Consider the square matrix*

$$X := \begin{bmatrix}A & 0\\ C & B\end{bmatrix} \tag{A.3}$$

*with $A \in \mathbb{R}^{n\times n}$, $B \in \mathbb{R}^{m\times m}$, and $C \in \mathbb{R}^{m\times n}$. Then*

$$\|X\|_{i2} \geq \max(\|A\|_{i2}, \|B\|_{i2}), \tag{A.4}$$

*where equality holds if and only if $C = 0$ (Bernstein, 2009).*

**Proof of Theorem 1.** First Statement A is proved. Convergence of the sequence of errors $\{\underline{e}_j^{\tau_j}\}_{j\in\mathbb{Z}_{\geq 0}}$ is equivalent to $\rho(I_{N^{\tau_0}} - \underline{J}_{\tau_0}\underline{L}_{\tau_0}) < 1$. From stabilizability, it is concluded that this is only possible if the pair $(A_e, B_e)$ is stabilizable. Since all eigenvalues of $A_e = I_{N^\tau}$ are 1, this is equivalent to controllability of the pair $(A_e, B_e) = (I_{N^\tau}, \underline{J}_\tau)$, i.e.,

$$\begin{aligned}\operatorname{rank}\left(\mathcal{C}_{S_e}\right) &= \operatorname{rank}\left(\begin{bmatrix}B_e & A_eB_e & \dots & A_e^{N^\tau-1}B_e\end{bmatrix}\right)\\ &= \operatorname{rank}(\underline{J}_\tau) = N^\tau,\end{aligned} \tag{A.5}$$

hence (32).

To prove Statement B, first note that a necessary condition to achieve monotonic convergence in any $p$-norm is to achieve convergence, since

$$\rho(X) \leq \|X\|_{ip}, \text{ for all } X \in \mathbb{R}^{n\times n}. \tag{A.6}$$

From this it follows that Condition (32) is a necessary condition to be able to design an ILC update (24) that achieves a monotonically convergent sequence of errors $\{e_j^\tau\}_{j\in\mathbb{Z}_{\geq 0}}$ in a given $p$-norm.

To show that (32) is also a sufficient condition, note that if Condition (32) is satisfied, the matrix $\underline{J}_\tau$ is full rank. This implies that there exists a matrix $\underline{L}_{\tau_0}$ such that $\|I_{N^\tau} - \underline{J}_{\tau_0}\underline{L}_{\tau_0}\|_{ip} < 1$, e.g., $\underline{L}_{\tau_0} = \underline{J}_{\tau_0}^{-1}$. Hence, Condition (32) is a necessary and sufficient condition to be able to design an ILC update (24) that achieves a monotonically convergent sequence of errors $\{e_j^{\tau_0}\}_{j\in\mathbb{Z}_{\geq 0}}$ in a given $p$-norm. This completes the proof.

**Proof of Theorem 2.** First statement A is proved. Convergence of the sequence of input signals $\{\underline{f}_j^l\}_{j\in\mathbb{Z}_{\geq 0}}$ is equivalent to the closed-loop dynamics (25) being stable. From detectability, it is concluded that this is only possible if the pair $(A_f, C_f)$ is detectable. Since all eigenvalues of $A_f$ are 1, this is equivalent to observability of the pair $(A_f, C_f)$. For the pair $(A_f, C_f) = (I_{N^l}, \underline{J}_\tau)$ the observability condition as given in Section 1.1 reduces to

$$\begin{aligned}\operatorname{rank}\left(\mathcal{O}_{S_f}\right) &= \operatorname{rank}\ker\left(\begin{bmatrix}C_f\\ C_fA_f\\ \vdots\\ C_fA_e^{N^\tau-1}\end{bmatrix}\right)\\ &= \operatorname{rank}(\ker(\underline{J}_\tau)) = 0.\end{aligned} \tag{A.7}$$

This proves Statement A.

The proof of Statement B follows similar reasoning as in the proof of Statement B of Theorem 1.

**Proof of Lemma 5.** This proof consists of two parts. In part 1 Condition (49) is derived from (25). In part 2 a state transformation of the system (22) is derived to decompose the state into an observable and unobservable part, this transformation is chosen such that the 2-norm of the input signal is preserved. The transformation of the closed-loop dynamics (25) yields conditions (48).

*Part 1:* Consider the closed-loop dynamics (25) for a given iteration $j$ with time-stamp sequence $\tau_j = \tau_0 \in \mathcal{T}$. From (25) it follows that Condition (47) is satisfied for iteration $j$ if and only if

$$\left\|I_{N^l} - \underline{L}_{\tau_j}\underline{J}_{\tau_j}\right\|_{i2} \leq 1. \tag{A.8}$$

Hence, Condition (47) is satisfied for each $j \in \mathbb{Z}_{\geq 0}$ if and only if Condition (49) is satisfied for all $\tau \in \mathcal{T}$.

*Part 2:* Consider an iteration $j$ with time-stamp sequence $\tau_j \in \mathcal{T}$ such that $\operatorname{rank}(\underline{J}_{\tau_j}) = N^{o_j} < N^l$, i.e., a part of the control input $\underline{f}_j^l$ is unobservable in the error $\underline{e}_j^{\tau_j}$. Hence, there exists a transformation

$$\begin{bmatrix}f_j^{l,o_j}\\ f_j^{l,uo_j}\end{bmatrix} = Y\underline{f}_j^l \tag{A.9}$$

such that

$$\begin{bmatrix}f_j^{l,o_j}\\ 0\end{bmatrix} = Y\underline{f}_{j,o_j}^l, \quad \begin{bmatrix}0\\ f_j^{l,uo_j}\end{bmatrix} = Y\underline{f}_{j,uo_j}^l, \tag{A.10}$$

with $\underline{f}_{j,o_j}^l$ and $\underline{f}_{j,uo_j}^l$ as in (45), and $f_j^{l,o_j} \in \mathbb{R}^{N^{o_j}}$ and $f_j^{l,uo_j} \in \mathbb{R}^{N^l-N^{o_j}}$. The transformation matrix $Y \in \mathbb{R}^{N^l\times N^l}$ is given by

$$Y = W^{-1} \text{ with } \left[w_1, \dots, w_{N^o}, w_{N^o+1}, \dots, w_{N^l}\right] \tag{A.11}$$

the columns $(w_{N^{o_j}+1}, \dots, w_{N^l})$ are linearly independent columns that span the unobservable space $\mathcal{O}_{S_f}$, and the vectors $(w_1, \dots, w_{N^{o_j}})$ are linear independent columns such that $W$ is nonsingular. Moreover, to preserve the 2-norm in this transformation, i.e.,

$$\left\|\begin{bmatrix}f_j^{l,o_j}\\ f_j^{l,uo_j}\end{bmatrix}\right\|_2 = \left\|\underline{f}_j^l\right\|_2 \tag{A.12}$$

$W$ is chosen to be a unitary matrix. To construct the matrix $W$ use the singular value decomposition of $\underline{J}_{\tau_j}$, given as follows

$$\underline{J}_{\tau_j} = \begin{bmatrix}U_{1,\tau_j} & U_{2,\tau_j}\end{bmatrix}\begin{bmatrix}\Sigma_{\tau_j} & 0\\ 0 & 0\end{bmatrix}\begin{bmatrix}V_{1,\tau_j}^T\\ V_{2,\tau_j}^T\end{bmatrix}^T \tag{A.13}$$

where $\begin{bmatrix}U_{1,\tau_j} & U_{2,\tau_j}\end{bmatrix} \in \mathbb{R}^{N^{\tau_j}\times N^{\tau_j}}$ is a unitary matrix, $\Sigma_{\tau_j}$ is a diagonal matrix with all $N^{o_j}$ singular values of $\underline{J}_{\tau_j}$, and $\begin{bmatrix}V_{1,\tau_j} & V_{2,\tau_j}\end{bmatrix} \in \mathbb{R}^{N^l\times N^l}$ is a unitary matrix. The columns of $V_{1,\tau_j} \in \mathbb{R}^{N^l\times N^{o_j}}$ provide an orthonormal basis of $\underline{J}_{\tau_j}$ and the columns of $V_{2,\tau_j} \in \mathbb{R}^{N^l \times (N^l - N^{o_j})}$ provide an orthonormal basis of ker $\left(\underline{J}_{\tau_j}\right)$, see Lemma 6. From this it follows that by choosing $W = V_{\tau_j}$, i.e., $Y = V_{\tau_j}^T$ a transformation (A.9) satisfying both (A.10) and (A.12) is obtained.

Using the transformation (A.9) the dynamics (22) are transformed into

$$\left[\begin{array}{c|c} V_{\tau_j}^T A_{f,\tau_j} V_{\tau_j} & V_{\tau_j}^T B_{f,\tau_j} \\ \hline C_{f,\tau_j} V_{\tau_j} & \end{array}\right] = \left[\begin{array}{cc|c} A_{f,\tau_j}^{11} & 0 & B_{f,\tau_j}^{o} \\ A_{f,\tau_j}^{21} & A_{f,\tau_j}^{22} & B_{f,\tau_j}^{uo} \\ \hline C_{f,\tau_j}^{o} & 0 & \end{array}\right] = \left[\begin{array}{cc|c} I_{N^{o_j}} & 0 & V_{1,\tau_j}^T \\ 0 & I_{N^l - N^{o_j}} & V_{2,\tau_j}^T \\ \hline -\underline{J}_{\tau_j} V_{1,\tau_j} & 0 & \end{array}\right]. \tag{A.14}$$

The corresponding transformed closed-loop dynamics (25) are given by

$$\begin{bmatrix} f_{j+1}^{l,o_j} \\ f_{j+1}^{l,uo_j} \end{bmatrix} = \begin{bmatrix} I_{N^l - N^{o_j}} - V_{1,\tau_j}^T \underline{L}_{\tau_j} \underline{J}_{\tau_j} V_{1,\tau_j} & 0 \\ V_{2,\tau_j}^T \underline{L}_{\tau_j} \underline{J}_{\tau_j} V_{1,\tau_j} & I_{N^o} \end{bmatrix} \begin{bmatrix} f_j^{l,o_j} \\ f_j^{l,uo_j} \end{bmatrix} \tag{A.15}$$

From this it follows that the observable part of the control input is updated according to

$$f_{j+1}^{l,o_j} = (I_{N^l - N^{o_j}} - V_{1,\tau_j}^T \underline{L}_{\tau_j} \underline{J}_{\tau_j} V_{1,\tau_j}) f_j^{l,o_j} \tag{A.16}$$

which shows that (46) is satisfied if and only if $\|(I_{N^l - N^{o_j}} - V_{1,\tau_j}^T \underline{L}_{\tau_j} \underline{J}_{\tau_j} V_{1,\tau_j})\|_{i2} < 1$. Hence, Condition (46) is satisfied for each $j \in \mathbb{Z}_{\geq 0}$ if and only if (48) is satisfied for each $\tau \in \mathcal{T}$. This completes the proof.

**Proof of Theorem 3.** This proof builds upon the state transformation (A.9) as introduced in the proof of Lemma 5.

From the transformed closed-loop dynamics (A.15) it follows that (47) is satisfied if and only if

$$\left\| \begin{bmatrix} I_{N^l - N^{o_j}} - V_{1,\tau}^T \underline{L}_\tau \underline{J}_\tau V_{1,\tau} & 0 \\ V_{2,\tau}^T \underline{L}_\tau \underline{J}_\tau V_{1,\tau} & I_{N^o} \end{bmatrix} \right\|_2 \leq 1, \tag{A.17}$$

for all $\tau \in \mathcal{T}$.

From Lemma 8 it follows that satisfying this condition for a given $\tau \in \mathcal{T}$ is equivalent to satisfying the following two conditions

$$V_{2,\tau}^T \underline{L}_\tau \underline{J}_\tau V_{1,\tau} = 0, \text{ and} \tag{A.18a}$$

$$\|I_{N^l - N^{o_j}} - V_{1,\tau}^T \underline{L}_\tau \underline{J}_\tau V_{1,\tau}\|_{i2} \leq 1, \tag{A.18b}$$

since $\|I_{N^o}\|_{i2} = 1$.

Since $\underline{J}_\tau V_{1,\tau}$ is full rank by construction, Condition (A.18a) is satisfied if and only if

$$V_{2,\tau}^T \underline{L}_\tau = 0 \tag{A.19}$$

Leading to the requirement

$$\underline{L}_\tau \in \ker(V_{2,\tau_j}^T) = \operatorname{im}(V_{1,\tau_j}^T) = \operatorname{im}(\underline{J}_{\tau_j}^T). \tag{A.20}$$

for each $\tau \in \mathcal{T}$.

From this it follows that by designing the matrices $\underline{L}_\tau$ such that for each $\tau \in \mathcal{T}$ condition (48) is satisfied, Condition (A.18b) and thereby Condition (49) is guaranteed. This completes the proof.

**Proof of Theorem 4.** Consider the finite-time ILC system (20) with desired output $\underline{y}_d^h$ satisfying Assumption 2. This proof consists of two parts. In the first part, it is shown that it is necessary to impose the structure (53) for some diagonal matrix $D$. In the second part, it is shown that the matrix $D$ should be designed to satisfy (54).

*Part 1*: To derive conditions on the structure of $\underline{L}_\tau$ first consider the sequences of measurement points $\tau_{1i} \in \mathcal{T}$ that consist of a single measurement point, i.e., $\tau_{1i} = (i)$, $i \in \{1, \dots, N_h\}$.

Notice that for each $\tau_{1i}$, $\underline{L}\underline{T}_{\tau_{1i}}$ results in a column vector, in particular the $i$th column of the matrix $\underline{L}$, i.e.,

$$\underline{L}\underline{T}_{\tau_{1i}} = \begin{bmatrix} \underline{L}_1 & \underline{L}_2 & \cdots & \underline{L}_{N_h} \end{bmatrix} \underline{T}_{\tau_{1i}} = \underline{L}_i. \tag{A.21}$$

Similar to this, for each $\tau_{1i}$, $(\underline{J}_{\tau_{1i}}^{h,l})^T \underline{T}_{\tau_{1i}}^T = (\underline{J}_i^{h,l})^T$ with $\underline{J}_i^{h,l}$ the $i$th row of the matrix $\underline{J}^{h,l}$. For each time-stamp sequence $\tau_{1i}, i \in \{1, 2, \dots, N_h\}$ this reduces (50) to $\underline{L}_i = d_i \underline{J}_i^{h,l^T}$, $d_i \in \mathbb{R}$. Hence, to satisfy (50) for each $\tau_{1i}, i \in \{1, 2, \dots, N_h\}$, a necessary structure for $\underline{L}$ is given by

$$\underline{L} = \begin{bmatrix} d_1 \underline{J}_1^{h,l^T} & d_2 \underline{J}_2^{h,l^T} & \cdots & d_{N_h} \underline{J}_{N_h}^{h,l^T} \end{bmatrix} = \underline{J}^{h,l^T} D \tag{A.22}$$

with $\underline{D} := \operatorname{diag}(d_1, d_2, \dots, d_{N_h})$.

To show that the structure (A.22) is also sufficient to guarantee Condition (50) for all $\tau \in \mathcal{T}$, first note that

$$\underline{D}\underline{T}_\tau^T = \underline{T}_\tau^T \underline{T}_\tau \underline{D}\underline{T}_\tau^T, \forall \tau \in \mathcal{T} \tag{A.23}$$

since the diagonal matrix $\underline{T}_\tau^T \underline{T}_\tau$ multiplies each $d_i$, $i \in \{1, \dots, N^h\}$ with 1, and all other elements with 0. Hence,

$$(\underline{J}^{h,l})^T \underline{D}\underline{T}_\tau^T = (\underline{J}^{h,l})^T \underline{T}_\tau^T \underline{T}_\tau \underline{D}\underline{T}_\tau^T = (\underline{J}^{h,l})^T \underline{T}_\tau^T X_\tau \tag{A.24}$$

with $X_\tau = \underline{T}_\tau \underline{D}\underline{T}_\tau^T$ for all $\tau \in \mathcal{T}$. This shows that imposing the structure (A.22) is necessary and sufficient to guarantee (50) for all $\tau \in \mathcal{T}$.

*Part 2:* From Theorem 3 it follows that the result of part 1 reduces the design problem of the ILC controller to finding a matrix $D$ that satisfies (48). Substituting the structure (53) into (48) leads to the condition

$$\|I_{N^l - N^o} - V_{1,\tau}^T \underbrace{\underline{J}^{h,l^T} D \underline{T}_\tau^T}_{\underline{L}_\tau = \underline{L}\underline{T}_\tau} \underbrace{\underline{T}_\tau \underline{J}^{h,l}}_{\underline{J}_\tau} V_{1,\tau}\|_{i2} < 1 \tag{A.25}$$

Since the matrix $I_{N^l - N^o} - V_{1,\tau_j}^T \underline{J}^{h,l^T} D \underline{T}_\tau^T \underline{T}_\tau \underline{J}^{h,l} V_{1,\tau_j}$ is symmetric,

$$\|I_{N^l - N^o} - V_{1,\tau_j}^T \underline{J}^{h,l^T} D \underline{T}_\tau^T \underline{T}_\tau \underline{J}^{h,l} V_{1,\tau_j}\|_{i2} = \rho(I_{N^l - N^o} - V_{1,\tau_j}^T \underline{J}^{h,l^T} D \underline{T}_\tau^T \underline{T}_\tau \underline{J}^{h,l} V_{1,\tau_j}) \tag{A.26}$$

for all $\tau \in \mathcal{T}$. This is equivalent to all eigenvalues being smaller than 1 and larger than -1, i.e., this condition is equivalent to satisfying both of the two LMIs

$$I_{N^l - N^o} - V_{1,\tau}^T \underline{J}^{h,l^T} D \underline{T}_\tau^T \underline{T}_\tau \underline{J}^{h,l} V_{1,\tau} \prec I_{N^l - N^o}, \tag{A.27a}$$

$$I_{N^l - N^o} - V_{1,\tau}^T \underline{J}^{h,l^T} D \underline{T}_\tau^T \underline{T}_\tau \underline{J}^{h,l} V_{1,\tau} \succ -I_{N^l - N^o}, \tag{A.27b}$$

for all $\tau \in \mathcal{T}$.

First, (A.23) is exploited to rewrite (A.27a) as

$$V_{1,\tau}^T \underline{J}^{h,l^T} \underline{T}_\tau^T \underline{T}_\tau D \underline{T}_\tau^T \underline{T}_\tau \underline{J}^{h,l} V_{1,\tau} \succ 0, \tag{A.28}$$

for all $\tau \in \mathcal{T}$. Because of the construction of the matrix $V_{1,\tau}$ through the singular value decomposition, the matrix $\underline{T}_\tau \underline{J}^{h,l} V_{1,\tau}$ is full rank and for the case where $\tau = \{1, \dots, N^h\}$ is of dimension $N^h \times N^h$. From Lemma 7 it is concluded that (A.27a) is satisfied if and only if the matrix $\underline{T}_\tau \underline{D}\underline{T}_\tau^T \succ 0$, for all $\tau \in \mathcal{T}$. Clearly this can only be satisfied if $d_i > 0$ for all $i \in \{1, 2, \dots, N_h\}$.

Next rewrite Condition (A.27b) as

$$V_{1,\tau}^T (2I_{N^l - N^o} - \underline{J}^{h,l^T} D \underline{T}_\tau^T \underline{T}_\tau \underline{J}^{h,l}) V_{1,\tau} \succ 0, \tag{A.29}$$

and, consider the situation where $\tau = \tau_N = \{1, \dots, N^h\}$, i.e., data is available at each time instance. In this case $\underline{T}_\tau^T \underline{T}_\tau = I_{N^h}$ which reduces Condition (A.29) to

$$V_{1,\tau_N}^T (2I_{N^l - N^o} - \underline{J}^{h,l^T} D \underline{J}^{h,l}) V_{1,\tau_N} \succ 0, \tag{A.30}$$

which is equivalent to condition (54) since $V_{1,\tau_N}$ is full-rank by design, this shows that Condition (54) is a necessary condition for the situation where all measurement data is available. To show that it is also a sufficient condition for all other time-stamp sequences note the following

$$\underline{T}_\tau D \underline{T}_\tau^T \preceq D \tag{A.31}$$

where the equality holds in the situation where $\tau = \{1, \ldots, N^h\}$, i.e., data is available at each time instance. Pre- and post multiplication with the full rank matrix $\underline{T}_\tau \underline{J}^{h,l} V_{1,\tau}$ yields

$$V_{1,\tau}^T \underline{J}^{h,l^T} \underline{T}_\tau^T \underline{T}_\tau D \underline{T}_\tau^T \underline{T}_\tau \underline{J}^{h,l} V_{1,\tau} \preceq V_{1,\tau}^T \underline{J}^{h,l^T} \underline{T}_\tau^T D \underline{T}_\tau \underline{J}^{h,l} V_{1,\tau} \tag{A.32}$$

Substituting this in (A.29) shows that

$$V_{1,\tau}^T (2I_{N^l-N^o} - \underline{J}^{h,l^T} D \underline{T}_\tau^T \underline{T}_\tau \underline{J}^{h,l}) V_{1,\tau} \succeq V_{1,\tau}^T (2I_{N^l-N^o} - \underline{J}^{h,l^T} D \underline{J}^{h,l}) V_{1,\tau} \succ 0, \tag{A.33}$$

for all $\tau \in \mathcal{T}$. Hence, Condition (A.27b) is satisfied for all $ts \in \mathcal{T}$ if and only if $2I_{N_l} - \underline{J}^{h,l^T} D \underline{J}^{h,l} \succ 0$, completing the proof.

## References


Ahn, H. S., Moore, K. L., & Chen, Y. Q. (2008). Discrete-time intermittent iterative learning controller with independent data dropouts. *IFAC Proceedings Volumes*, *41*(2), 12442–12447, 17th IFAC World Congress.

Altın, B., & Sanfelice, R. G. (2018). Model predictive control under intermittent measurements due to computational constraints: Feasibility, stability, and robustness. In *2018 annual american control conference (ACC)* (pp. 1418–1423).

Amann, N., Owens, D., & Rogers, E. (1996). Iterative learning control for discrete-time-systems with exponential rate of convergence. *IEE Proceedings - Control Theory and Applications*, *143*(2), 217–224.

Barton, K. L., & Alleyne, A. G. (2011). A norm optimal approach to time-varying ILC with application to a multi-axis robotic testbed. *IEEE Transactions on Control Systems Technology*, *19*(1), 166–180.

Barton, K. L., Hoelzle, D. J., Alleyne, A. G., & Johnson, A. J. W. (2011). Cross-coupled iterative learning control of systems with dissimilar dynamics: design and implementation. *International Journal of Control*, *84*(7), 1223–1233.

Bernstein, D. S. (2009). *Matrix mathematics: theory, facts, and formulas*. Princeton University Press.

Blanken, L., van Zundert, J., de Rozario, R., Strijbosch, N., & Oomen, T. (2019). In S. Formentin, & C. Novara (Eds.), *Application-oriented system identification: prediction, filtering and control*.

Bolder, J., Kleinendorst, S., & Oomen, T. Data-driven multivariable ILC: enhanced performance by eliminating l and q filters. *International Journal of Robust and Nonlinear Control*, *28*(12), 3728–3751.

Bolder, J., & Oomen, T. (2016). Inferential iterative learning control: A 2D-system approach. *Automatica*, *71*, 247–253.

Bolder, J., Oomen, T., Koekebakker, S., & Steinbuch, M. (2014). Using iterative learning control with basis functions to compensate medium deformation in a wide-format inkjet printer. *Mechatronics*, *24*(8), 944–953.

Bristow, D. A., Tharayil, M., & Alleyne, A. G. (2006). A survey of iterative learning control. *IEEE Control Systems Magazgine*, *26*(3), 96–114.

Chu, B., & Owens, D. H. (2009). Accelerated norm-optimal iterative learning control algorithms using successive projection. *International Journal of Control*, *82*(8), 1469–1484.

Dan, G., & Sandberg, H. (2010). Stealth attacks and protection schemes for state estimators in power systems. In *2010 First IEEE international conference on smart grid communications* (pp. 214–219).

Frueh, J. A., & Phan, M. Q. (2000). Linear quadratic optimal learning control (LQL). *International Journal of Control*, *73*(10), 832–839.

Hoelzle, D. J., Alleyne, A. G., & Johnson, A. J. W. (2010). Basis task approach to iterative learning control with applications to micro-robotic deposition. *IEEE Transactions on Control Systems Technology*, *19*(5), 1138–1148.

Longman, R. W. (2000). Iterative learning control and repetitive control for engineering practice. *International Journal of Control*, *73*(10), 930–954.

Merry, R. J. E., van de Molengraft, M. J. G., & Steinbuch, M. (2013). Optimal higher-order encoder time-stamping. *Mechatronics*, *23*(5), 481–490.

Mishra, S., Coaplen, J., & Tomizuka, M. (2007). Precision positioning of wafer scanners segmented iterative learning control for nonrepetitive disturbances. *IEEE Control Systems Magazine*, *27*(4), 20–25.

Oomen, T., & Rojas, C. R. (2017). Sparse iterative learning control with application to a wafer stage: Achieving performance, resource efficiency, and task flexibility. *Mechatronics*, *47*, 134–147.

Oomen, T., van de Wijdeven, J., & Bosgra, O. (2009). Suppressing intersample behavior in iterative learning control. *Automatica*, *45*(4), 981–988.

Owens, D. H., Hatonen, J. J., & Daley, S. (2009). Robust monotone gradient-based discrete-time iterative learning control. *International Journal of Robust and Nonlinear Control: IFAC-Affiliated Journal*, *19*(6), 634–661.

Paszke, W., Rogers, E., Gałkowski, K., & Cai, Z. (2013). Robust finite frequency range iterative learning control design and experimental verification. *Control Engineering Practice*, *21*(10), 1310–1320.

Phan, M., & Longman, R. (1988). A mathematical theory of learning control for linear discrete multivariable systems. In *Astrodynamics conference* (p. 4313).

Salton, A. T., Fu, M., Flores, J. V., & Zheng, J. (2020). High precision over long range: A macro-micro approach to quantized positioning systems. *IEEE Transactions on Control Systems Technology*, 1–10.

Seel, T., Schauer, T., & Raisch, J. (2011). Iterative learning control for variable pass length systems. *IFAC Proceedings Volumes*, *44*(1), 4880–4885, 18th IFAC World Congress.

Shen, D. (2018). Iterative learning control with incomplete information: A survey. *IEEE/CAA Journal of Automatica Sinica*, *5*(5), 885–901.

Shen, D., & Wang, Y. (2015a). ILC for networked nonlinear systems with unknown control direction through random lossy channel. *Systems & Control Letters*, *77*, 30–39.

Shen, D., & Wang, Y. (2015b). Iterative learning control for networked stochastic systems with random packet losses. *International Journal of Control*, *88*(5), 959–968.

Skogestad, S., & Postlethwaite, I. (2007). *vol. 2*, *Multivariable feedback control: analysis and design*. Wiley New York.

Son, T. D., Pipeleers, G., & Swevers, J. (2016). Robust monotonic convergent iterative learning control. *IEEE Transactions on Automatic Control*, *61*(4), 1063–1068.

Strijbosch, N., & Oomen, T. (2019a). Beyond quantization in iterative learning control: Exploiting time-varying time-stamps. In *American control conference 2019*. Philadelphia, USA.

Strijbosch, N., & Oomen, T. (2019b). Intermittent sampling in iterative learning control: a monotonically-convergent gradient-descent approach with application to time stamping. In *2019 IEEE 58th conference on decision and control (CDC)* (pp. 6542–6547). IEEE.

Strijbosch, N., Tacx, P., Verschueren, E., & Oomen, T. (2019). Commutation angle iterative learning control: enhancing piezo-stepper actuator waveforms. *IFAC-PapersOnLine*, *52*(15), 579–584.

Svante, G., & Norrlöf, M. (2001). On the design of ILC algorithms using optimization. *Automatica*, *37*(12), 2011–2016.

van der Meulen, S. H., Tousain, R. L., & Bosgra, O. H. (2008). Fixed structure feedforward controller design exploiting iterative trials: Application to a wafer stage and a desktop printer. *Journal of Dynamic Systems, Measurement, and Control*, *130*(5).

Wallén, J., Norrlöf, M., & Gunnarsson, S. (2011). A framework for analysis of observer-based ILC. *Asian Journal of Control*, *13*(1), 3–14.

Zhou, K., Doyle, J. C., & Glover, K. (1996). *Robust and optimal control*. Prentice hall New Jersey.


**Nard Strijbosch** received both his B.Sc. degree (cum laude) and M.Sc. degree (cum laude) from the Eindhoven University of Technology, Eindhoven, The Netherlands. He is currently a Ph.D. candidate at the Eindhoven University of Technology. He is a recipient of the IEEJ Industry Applications Society Excellent Presentation Award (SAMCON 2018). His research interest is in the field of motion control and learning control techniques for applications in mechatronic systems.

**Tom Oomen** received the M.Sc. degree (cum laude) and Ph.D. degree from the Eindhoven University of Technology, Eindhoven, The Netherlands. He is currently a professor with the Department of Mechanical Engineering at the Eindhoven University of Technology. He is also a part-time full professor with the Delft University of Technology. He held visiting positions at KTH, Stockholm, Sweden, and at The University of Newcastle, Australia. He is a recipient of the 7th Grand Nagamori Award, the Corus Young Talent Graduation Award, the IFAC 2019 TC 4.2 Mechatronics Young Research Award, the 2015 IEEE Transactions on Control Systems Technology Outstanding Paper Award, the 2017 IFAC Mechatronics Best Paper Award, the 2019 IEEJ Journal of Industry Applications Best Paper Award, and recipient of a Veni and Vidi personal grant. He is Associate Editor of the IEEE Control Systems Letters (L-CSS), IFAC Mechatronics, and IEEE Transactions on Control Systems Technology. He is a member of the Eindhoven Young Academy of Engineering. His research interests are in the field of data-driven modelling, learning, and control, with applications in precision mechatronics.